



HAL
open science

Serum Albumin Antifouling Effects of Hydroxypropylcellulose and Pluronic F127 Adsorbed on Isobutyramidegrafted Stellate Silica Nanoparticles

Joëlle Bizeau, Alexandre Adam, Sylvie Bégin-Colin, Damien Mertz

► **To cite this version:**

Joëlle Bizeau, Alexandre Adam, Sylvie Bégin-Colin, Damien Mertz. Serum Albumin Antifouling Effects of Hydroxypropylcellulose and Pluronic F127 Adsorbed on Isobutyramidegrafted Stellate Silica Nanoparticles. *European Journal of Inorganic Chemistry*, 2021, 2021 (46), pp.4799-4805. 10.1002/ejic.202100678 . hal-03872451

HAL Id: hal-03872451

<https://hal.science/hal-03872451>

Submitted on 25 Nov 2022

HAL is a multi-disciplinary open access archive for the deposit and dissemination of scientific research documents, whether they are published or not. The documents may come from teaching and research institutions in France or abroad, or from public or private research centers.

L'archive ouverte pluridisciplinaire **HAL**, est destinée au dépôt et à la diffusion de documents scientifiques de niveau recherche, publiés ou non, émanant des établissements d'enseignement et de recherche français ou étrangers, des laboratoires publics ou privés.

Serum Albumin Antifouling Effects of Hydroxypropyl-cellulose and Pluronic F127 Adsorbed on Isobutyramide-grafted Stellate Silica Nanoparticles

Ms Joëlle Bizeau¹, Mr Alexandre Adam¹, Prof. Dr. Sylvie Bégin¹, Dr Damien Mertz^{1,*}

¹Institut de Physique et Chimie des Matériaux de Strasbourg (IPCMS), UMR-7504 CNRS-Université de Strasbourg, 23 rue du Loëss, BP 34 67034, Strasbourg Cedex 2, France.

E-mail : damien.mertz@ipcms.unistra.fr

Abstract

Limiting the serum protein fouling is a major challenge in the design of nanoparticles (NPs) for nanomedicine applications. Suitable chemical surface modification strategies allow to limit the interactions with adsorbing proteins. In this communication, we address the potential of isobutyramide (IBAM) groups grafted on stellate silica nanoparticles (STMS) for the immobilization of two biocompatible polymers renowned for biomedical and low fouling applications: Hydroxypropylcellulose (HPC) and Pluronic F127 (PF127). We report that both polymers can be loaded on STMS@IBAM NPs surface with a maximum loading content close to 10 wt %. Regarding their antifouling properties, we report that the coatings of such HPC or PF127 polymers allow to reduce significantly the human serum albumin (HSA) adsorption in average by 70 % as compared to the surface of the free polymer STMS@IBAM. These results highlight the antifouling potential of these polymer pre-treatments on IBAM-modified STMS NPs surface.

1 Introduction

An important challenge in medical research is to design specific delivery systems that can target the injured site in a human body and release their therapeutic cargo in a controlled way. Recently, in our team, we have developed an interface based on isobutyramide (IBAM) groups grafted on the surface of mesoporous silica (MS) nanoparticles (NPs) or MS shelled iron oxide or carbon nanotubes which allow to adsorb a whole range of bioactive (antitumor) molecules (Doxorubicin, curcumin, camptothecin^[1,2]) and biopolymers including proteins^[3,4], polysaccharides^[5], DNA/RNA^[6,7]. The IBAM groups were grafted in two sequential steps: one step with aminosilane (APTES) and then conversion of amine groups in IBAM through reaction with isobutrylchloride (IBC). As suitable MS substrate for these binders, we used large pore MS silica named stellate MS (STMS) which display high surface area (ca. 500 m².g⁻¹) and pore size of ca. 10-15 nm whose initial synthesis was described by Zhang *et al*^[8]. Such STMS were recently functionalized with various inorganic NPs (quantum dots, iron oxide)^[9] for bimodal imaging combined to magnetic hyperthermia or grafted with high affinity ligand for iron removal in brain mimicking fluid^[10].

However, given the strong affinity of IBAM surface observed with many proteins, and in particular serum albumin, it is anticipated that a protein corona will form around these NPs when used for biomedical application. Indeed, it is now well-known that when NPs are introduced in a biological fluid, they interact with biomolecules and a protein corona ultimately forms at its surface. This protein corona gives a new biological identity to the NPs, and thus has an impact on its interactions with the other biomolecules and cells. Unfortunately, the protein bounding on the NPs surface can lead to the conformational change of these proteins, which then may lead to harmful side effects, for example due to the activation of an undesired cell signaling pathway^[11–15]. Limiting the protein corona formation is thus a major challenge in the surface design of NPs for nanomedicine applications.

Aside features such as size, shape and charge, the chemical surface modification of an NP is a key aspect which determines the interactions of adsorbing proteins, and thus can be used to control it^[13–15]. Among existing chemical strategies, there are efficient approaches to ensure antifouling properties involving mainly the pegylation (and dendronization) or the use of zwitterion polymers which are probably the main reported ways to date^[15–17]. The introduction of such moieties can be afforded essentially by covalent grafting at the surface of various types of NPs such as quantum dots^[18] or iron oxide NPs^[19]. One of the main limitations of the covalent grafting is that it usually involves a multi-step synthesis procedure either at the NP surface or in the preformed polymer. To avoid the use of complex procedures or even the introduction of potentially harmful molecules at NPs surface, other methods used the direct coating/adsorption of polymer but the coating instability may preclude the antifouling effect once the polymer is desorbed.

As said previously, the IBAM group allows the high adsorption of a variety of biomolecules on NPs, which will highly probably lead to the formation of a protein corona. But this high adsorbing property could also be exploited to coat the NPs with antifouling polymers by simple adsorption, without the need to chemically modify the polymers, expanding considerably the range of potential functional polymers for this coating. In addition, this would be an extremely simple and tunable way to enable stealth properties without the need for surface linkers that could be harmful for the different potential cargos (drug, ligand, probes etc..).

Among the potential polymers, Hydroxypropylcellulose (HPC) and Pluronic F127 (PF127) appear as two polymers of interest for several reasons: they are both biocompatible, inexpensive and thermoresponsive, this latter being an interesting property that can be used to deliver active principles by hyperthermia. Indeed, HPC displays a Lower Critical Solution Temperature (LCST) at 41°C^[20–22]. This LCST ensures HPC to be in its expanded, hydrophilic state at physiological temperature, limiting the protein adsorption^[16,23,24]. Regarding PF127, its LCST at 37°C has been exploited to form *in situ* gel at physiological pH^[20,25,26] and its antifouling properties due to the hydrophilicity of its polyethylene oxide groups were well studied and used to improve membrane low fouling^[27–29].

Herein, we report for the first time the adsorption study of HPC and PF127 polymers on STMS@IBAM NPs surface. The amount adsorbed in aqueous solution of each polymer is investigated as a function of their concentration (or feed weight ratio (FWR)) by thermogravimetric analysis (TGA). Next, with the aim to assess the antifouling potential of these polymer-coated NPs, the adsorption of human serum

albumin (HSA) in the presence or in the absence of the polymer layer are evaluated and compared. The HSA adsorption study is achieved by spectrofluorimetry using intrinsic fluorescence of the HSA tryptophan. HSA is known to adsorb with a very rapid kinetics and with a very high loading capacity (LC) at the surface of STMS@IBAM (*ca.* 442 $\mu\text{g}\cdot\text{mg}^{-1}$). We address herein the effects of the pre-adsorbed polymers at the STMS@IBAM surface to significantly limit the final amount of adsorbed HSA. Such an effect, which was never reported up to date, may allow to develop new antifouling properties towards HSA or other serum proteins. Figure 1 represents a global view of the study.

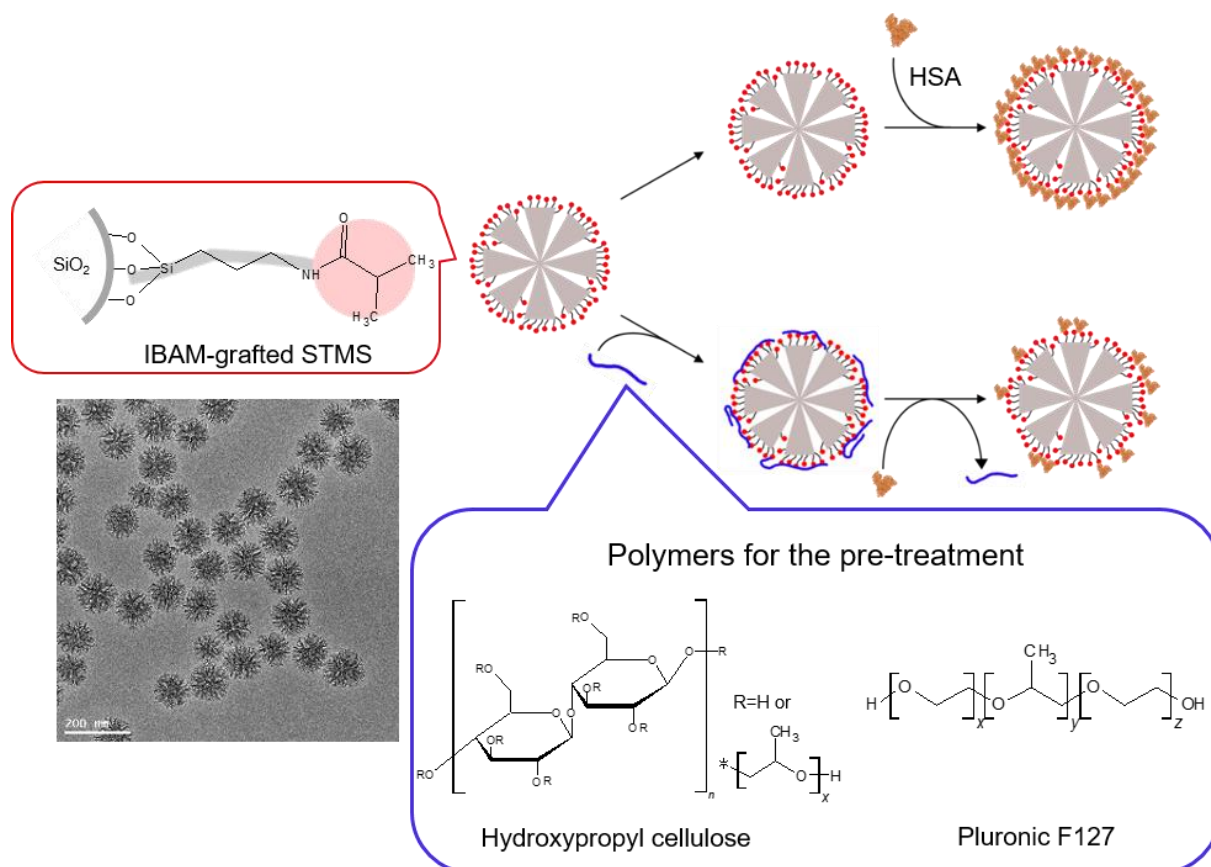


Figure 1: Representative scheme of the HSA adsorption on STMS@IBAM without and with a polymer pre-treatment

2 Results and discussion

The first objective of this work was to investigate the adsorption of the two chosen polymers: HPC and PF127 individually on the surface of STMS@IBAM NPs. The chemical functionalization of STMS with APTES and IBAM groups was done following the usual protocol described in the experimental section in Supporting information. First, the STMS was functionalized with APTES to add amines on the particle surface, and then these amines reacted with IBC to obtain the IBAM groups. TGA analysis was used to quantify the amount of grafted APTES and IBAM as it gives access to the total amount of organic material per mass of inorganic material (STMS). Thus the quantity of organic material present at the surface of STMS was

calculated as given in Eq. 1. The amount of the last molecule grafted or adsorbed was then calculated by subtracting the quantity of organic material from the previous layer. A more detailed explanation of the calculations is also presented in Figure S1.

$$\text{Quantity of organic material } (\mu\text{g. mg}_{\text{STMS}}^{-1}) = 1000 * \frac{\%W_{t_{100^{\circ}\text{C}}} - \%W_{t_{780^{\circ}\text{C}}}}{\%W_{t_{780^{\circ}\text{C}}}} \text{ (Eq. 1)}$$

Results (Figure S2) indicate that APTES grafting accounts for $93.5 \mu\text{g. mg}^{-1}$ ($1.9 / \text{nm}^2$) and IBAM moieties account for $131.1 \mu\text{g. mg}^{-1}$ ($2.3 / \text{nm}^2$) which is in agreement with previous works^[5,10].

Then, the adsorption of each polymer was performed with several FWRs (Eq. 2), which was defined as:

$$\text{FWR} = 100 * \frac{m_{\text{polymer}}}{m_{\text{STMS}}} \text{ (Eq 2)}$$

TGA was also used to quantify the amount of adsorbed polymer, with typical representative curves presented in Figure 2.A (HPC) and Figure 2.B (PF127), and the same calculations than for APTES and IBAM were applied to obtain the LC in polymer. The LC is defined in μg of polymer per mg of unmodified STMS. The averaged results are presented in Figure 2.C for HPC and Figure 2.D for PF127. They show that, for both polymers, we could modulate the LC by playing on the FWR. A maximum LC of $97 \mu\text{g. mg}^{-1}$ was reached for HPC from a FWR of 25 % while a minimum FWR of 75 % was necessary to reach the maximum LC of PF127, which was $90 \mu\text{g. mg}^{-1}$. The binding interaction of these polymer coatings is hypothesized to occur through hydrogen bonding between the IBAM (amide) groups and the HPC and PF127 polymers containing respectively OH or ether groups as reported previously^[7]. Indeed, aside the coating of proteins, IBAM groups were reported to non-covalently bind various polysaccharides such as dextran yielding to self-supported microcapsules^[7] or chitosan to form protective nanocoating towards heavy metal diffusion^[5].

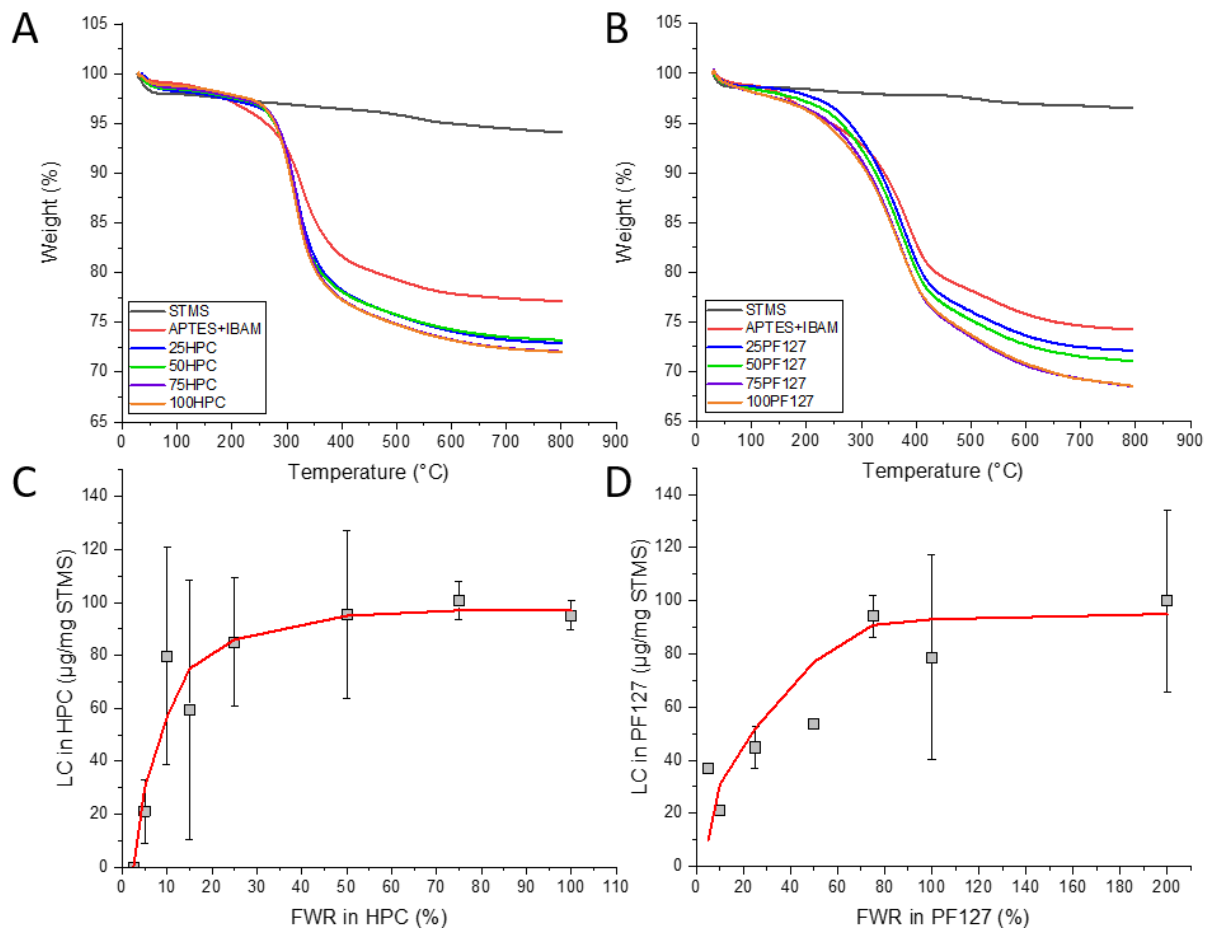


Figure 2: A) and B): TGA curves of bare STMS (dark lines), STMS@IBAM (red lines), STMS@IBAM@25polymer (bleu lines), STMS@IBAM@50polymer (green lines), STMS@IBAM@75polymer (purple lines) and STMS@IBAM@100polymer (orange lines) with “polymer” being HPC in A) and PF127 in B) and the number being the FWR in polymer. C) and D): LC in C) HPC and D) PF127 after adsorption on STMS@IBAM with different FWR in polymer (red lines show the general tendency).

Then, the adsorption of HSA on these two polymer-coated STMS@IBAM was studied in order to evaluate their antifouling properties. To do so, the FWR in HSA was fixed at 40 % for all experiments as it leads to a high LC on STMS@IBAM and thus offers a good control sample to investigate the low fouling effect. The LC in HSA was evaluated indirectly by exploiting the intrinsic fluorescence of HSA due to its tryptophan residue ($\lambda_{exc}/\lambda_{em} = 295/337$ nm). Fluorescence spectroscopy was thus used to measure the HSA concentration in the supernatants collected after adsorption. A typical fluorescence curve and the calibration curve are presented in Figure 3.A and B respectively. The adsorption results are presented in Figure 3.C (HPC) and Figure 3.D (PF127). In this case, the LC in HSA was calculated with Eq 3:

$$LC = \frac{m_{HSA}}{m_{STMS}} \quad (\text{Eq 3})$$

with m_{HSA} the mass of adsorbed HSA determined by fluorescence, and m_{STMS} the mass of unmodified STMS. As expected, the LC in HSA, which is ca. $442 \mu\text{g} \cdot \text{mg}^{-1}$

when adsorbed on STMS@IBAM, was highly reduced in the presence of both HPC and PF127, without any correlation between the amount of polymer and the final LC in HSA. Indeed, the lowest amount of HPC led to a reduction of the LC of HSA of ca. 66 % while the highest amount led to a reduction of ca. 82%. In the range of the LC used, the presence of HPC reduced the adsorption of HSA by ca. 71 % in average. Regarding PF127, the lowest amount of polymer reduced the adsorption of HSA by ca. 72 % and the highest amount by ca. 71 %. In the range of the LC used, the average HSA reduced adsorption was ca. 69% for this polymer. These results show that the coating of STMS@IBAM with HPC or PF127 can effectively reduce the adsorbing property of these particles toward HSA into an antifouling property, even with a low quantity of polymer.

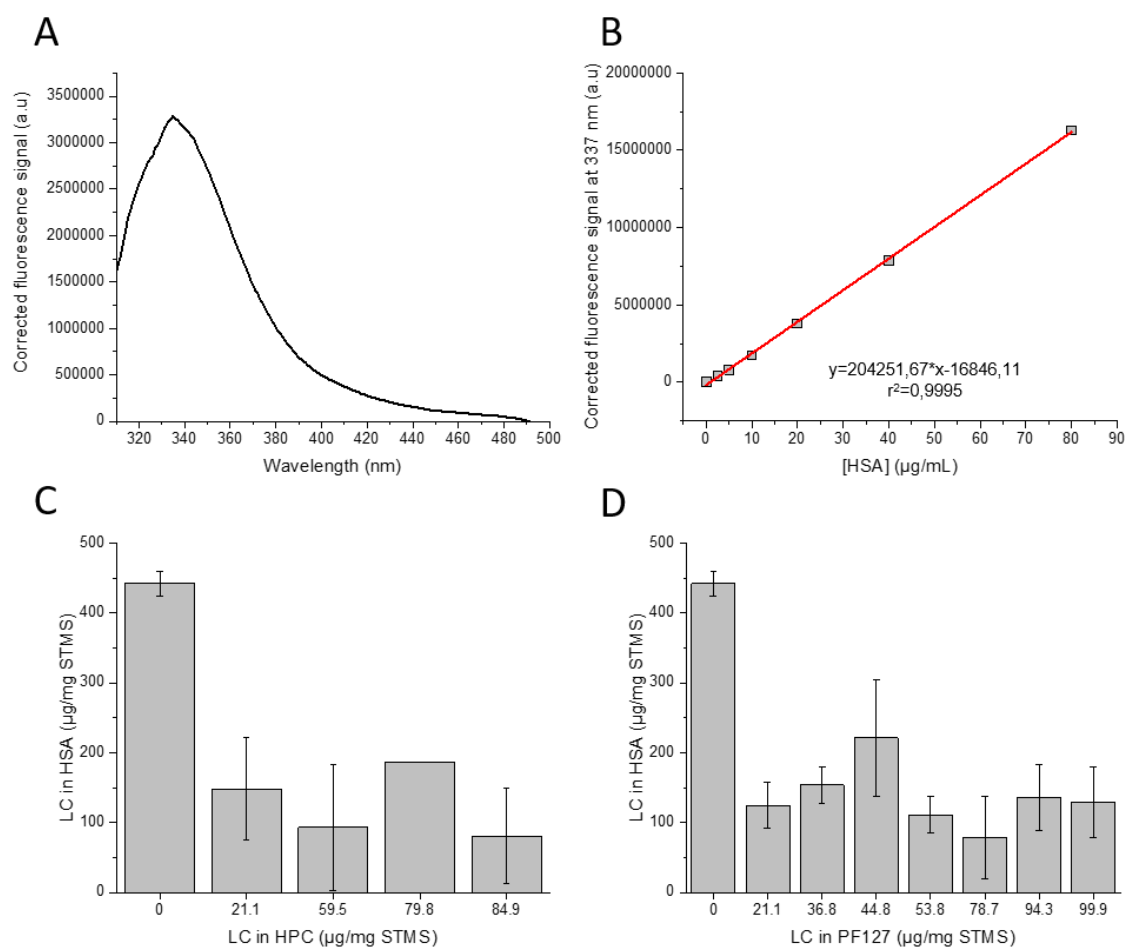


Figure 3: A) Representing fluorescence spectra of supernatant collected after the adsorption of HSA on STMS@IBAM@xpolymer. B) Calibration curve of HSA in water representing the maximum fluorescence of tryptophan residues at 337 nm in function of HSA concentration. C) and D): LC in HSA obtained with a constant FWR of 40% in HSA on C) STMS@IBAM@xHPC with x being the LC in HPC and on D) STMS@IBAM@yPF127 with y being the LC in PF127

TGA was also performed after the HSA adsorption to confirm the coating with a direct analysis. Surprisingly, TGA curves after HSA adsorption showed a total weight loss that was not higher than before HSA adsorption, as expected, but was slightly lower as it can be seen in Figure 4. These results indicate that for both polymers, a

loss of material occurred during this HSA adsorption step. If we examine the difference between the final % wt and the % wt after elimination of all the remaining solvents, we can see that the difference is quite similar between the samples before and after HSA adsorption: ca. 26.2 % before adsorption versus ca. 25.3 % after for HPC and ca. 27.9 % before versus ca. 23.4% after for PF127. This means that the total quantity of organic material is similar before and after adsorption. Furthermore, the previous experiments showed a maximum polymer loading of ca. 97 and 90 $\mu\text{g}\cdot\text{mg}^{-1}$ for HPC and PF127 respectively obtained by TGA, and a final amount of adsorbed HSA of ca. 127 and 136 $\mu\text{g}\cdot\text{mg}^{-1}$ in average, respectively, obtained by fluorimetry. As these amounts are relatively close, and taking into consideration that the polymers are adsorbed on the STMS@IBAM and not covalently attached to it, we suggest that the loss of material observed with the TGA curves of Figure 4 corresponds to the removal of the polymer from the particles surface and its replacement by HSA during the HSA adsorption.

As a control experiment, and to validate that any polymer release does not influence our method for the HSA fluorimetric quantification, we checked that the fluorescence of HSA could not be influenced by the presence of polymer in the supernatants, as the tryptophan fluorescence is sensitive to its environment. This was checked by measuring the fluorescence of HSA in presence of polymer in the same ratio than when adsorbing HSA on STMS@IBAM@xpolymer. The results (presented in Figure S3) showed no effect on the fluorescence, which allowed us to still validate our previous HSA LC results. Thus, we can speak about a pre-treatment of the particles surface with polymers leading to the modification of its adsorbing properties toward HSA.

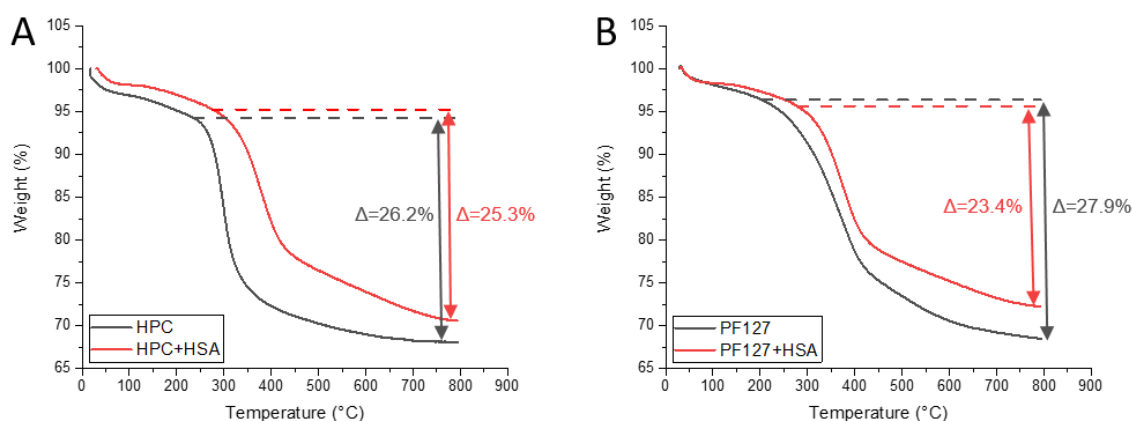


Figure 4: TGA curves of STMS@IBAM@xpolymer (black lines) and STMS@IBAM@xpolymer@40HSA (red lines) with x being in A) the FWR in HPC, here 15%, and in B) the FWR in PF127, here 75%.

The colloidal stability at pH 7.4 of the particles before and after HSA adsorption has been checked for each polymer with an FWR leading to the highest LC in polymer: 25% for HPC and 100% for PF127. The DLS results are presented in Figure 5 and the zeta potential is reported in Table 1. As it can be seen, the particles coated with HPC are overall well dispersed however they tend to form some slight

aggregates of several micron size, which may be explained by the zeta potential, not high enough in absolute value to provide sufficient electrostatic repulsion between particles. Thereafter, the adsorption of HSA tends to stabilize the particles as there is less aggregates. In any way, it does not decrease the colloidal stability. Regarding the particles coated with PF127, they are very stable before and after HSA adsorption, with a small increase of the hydrodynamic diameter after adsorption. This study has also been conducted with lower FWRs (5% for HPC and 25% for PF127). The results reported in Figure S4 and Table S1 with lower FWRs gave similar results as described above. These results suggest that PF127 is a better choice as it shows a better colloidal stability.

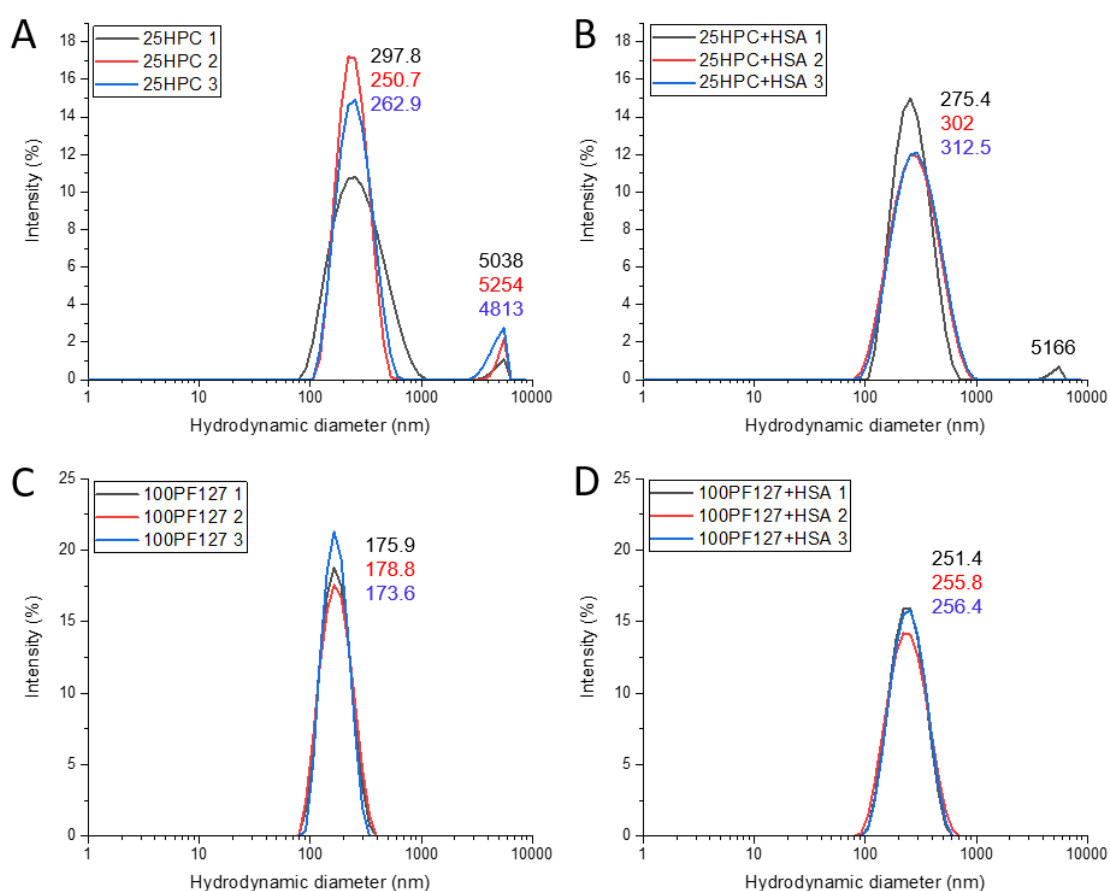


Figure 5: DLS measurements in triplicate for A) STMS@IBAM@25HPC, B) STMS@IBAM@25HPC@HSA, C) STMS@IBAM@100PF127 and D) STMS@IBAM@100PF127@HSA

Table 1: Zeta potential of the polymer-coated STMS@IBAM before and after HSA adsorption

Surface	25HPC	25HPC+HSA	100PF127	100PF127+HSA
Zeta potential	7.21	-6.56	11.63	-18.70
STD (mV)	±0.34	±0.66	±0.57	±1.11

3 Conclusions

In this work, we have investigated the adsorption of HPC and PF127, two well-established polymers renowned for biomedical applications, on IBAM-modified STMS NPs surface. We achieved adsorption curves as a function of their FWR and showed that both polymers can be loaded with a maximum loading content close to ca. 10% wt (LC of ca. 97 and 90 $\mu\text{g}\cdot\text{mg}^{-1}$ STMS for HPC and PF127, respectively).

Regarding HSA adsorption studies, we showed that such HPC or PF127 polymer pre-coatings, even with few deposited amounts, were able to reduce significantly the HSA adsorption in average by ca. 71 % for HPC and 69 % for PF127, as compared to the high loading content at the surface of the free polymer STMS@IBAM (442 $\mu\text{g}\cdot\text{mg}^{-1}$). Regarding the mechanism involved at NPs surfaces, TGA experiments before and after HSA adsorption suggests removal of the polymers after HSA adsorption.

Overall, these results emphasize the antifouling potential of these polymer-pre-treatment on IBAM-modified STMS NPs surface to significantly limit the final amount of adsorbed HSA. Such strategies may be useful in the future as an alternative to current antifouling strategy to limit the fouling of serum proteins involved in the protein corona formation.

Acknowledgements. D.M. acknowledges the Materials Institute Carnot Alsace (project ProtRemote), and the Agence Nationale de la Recherche (grant ANR-19-CE09-0004—Corelmag) for financial supports. The spectroscopy and the transmission electronic microscopy platforms of the IPCMS are acknowledged for technical supports. D. Burger, B. Li, L. Kelhetter and G. Cotin are thanked for their helps and discussions with TGA. D. Cianfarani is thanked for his help with fluorimeter.

Keywords: Biopolymers, Mesoporous materials, Nanoparticles, Protein corona, Serum protein antifouling/Antifouling

References

- [1] B. Li, S. Harlepp, V. Gensbittel, C. J. R. Wells, O. Bringel, J. G. Goetz, S. Bégin-Colin, M. Tasso, D. Bégin, D. Mertz, *Materials Today Chemistry* **2020**, *17*, 100308.
- [2] V. Fiegel, S. Harlepp, S. Bégin-Colin, D. Bégin, D. Mertz, *Chemistry – A European Journal* **2018**, *24*, 4662–4670.
- [3] D. Mertz, J. Cui, Y. Yan, G. Devlin, C. Chaubaroux, A. Dochter, R. Alles, P. Lavalle, J. C. Voegel, A. Blencowe, P. Auffinger, F. Caruso, *ACS Nano* **2012**, *6*, 7584–7594.
- [4] D. Mertz, H. Wu, J. S. Wong, J. Cui, P. Tan, R. Alles, F. Caruso, *J. Mater. Chem.* **2012**, *22*, 21434–21442.
- [5] F. Perton, S. Harlepp, G. Follain, K. Parkhomenko, J. G. Goetz, S. Bégin-Colin, D. Mertz, *Journal of Colloid and Interface Science* **2019**, *542*, 469–482.

- [6] D. Mertz, C. Affolter-Zbaraszczyk, J. Barthès, J. Cui, F. Caruso, T. F. Baumert, J.-C. Voegel, J. Ogier, F. Meyer, *Nanoscale* **2014**, *6*, 11676–11680.
- [7] D. Mertz, P. Tan, Y. Wang, T. K. Goh, A. Blencowe, F. Caruso, *Advanced Materials* **2011**, *23*, 5668–5673.
- [8] K. Zhang, L.-L. Xu, J.-G. Jiang, N. Calin, K.-F. Lam, S.-J. Zhang, H.-H. Wu, G.-D. Wu, B. Albel, L. Bonneviot, P. Wu, *J. Am. Chem. Soc.* **2013**, *135*, 2427–2430.
- [9] F. Pertont, M. Tasso, G. A. Muñoz Medina, M. Ménard, C. Blanco-Andujar, E. Portiansky, M. B. F. van Raap, D. Bégin, F. Meyer, S. Begin-Colin, D. Mertz, *Applied Materials Today* **2019**, *16*, 301–314.
- [10] P. Duenas-Ramirez, C. Bertagnolli, R. Müller, K. Sartori, A. Boos, M. Elhabiri, S. Bégin-Colin, D. Mertz, *Journal of Colloid and Interface Science* **2020**, *579*, 140–151.
- [11] M. Mahmoudi, I. Lynch, M. R. Ejtehadi, M. P. Monopoli, F. B. Bombelli, S. Laurent, *Chem. Rev.* **2011**, *111*, 5610–5637.
- [12] Q. Mu, G. Jiang, L. Chen, H. Zhou, D. Fourches, A. Tropsha, B. Yan, *Chem Rev* **2014**, *114*, 7740–7781.
- [13] M. Lundqvist, I. Sethson, B.-H. Jonsson, *Langmuir* **2004**, *20*, 10639–10647.
- [14] S. Devineau, L. Zargarian, J.-P. Renault, S. Pin, *Langmuir* **2017**, *33*, 3241.
- [15] N. Singh, C. Marets, J. Boudon, N. Millot, L. Saviot, L. Maurizi, *Nanoscale Advances* **2021**, *3*, 1209–1229.
- [16] D. Rana, T. Matsuura, *Chem. Rev.* **2010**, *110*, 2448–2471.
- [17] P. Bevilacqua, S. Nuzzo, E. Torino, G. Condorelli, M. Salvatore, A. M. Grimaldi, *Nanomaterials* **2021**, *11*, 780.
- [18] M. Tasso, E. Giovanelli, D. Zala, S. Bouccara, A. Fragola, M. Hanafi, Z. Lenkei, T. Pons, N. Lequeux, *ACS Nano* **2015**, *9*, 11479–11489.
- [19] G. Cotin, C. Blanco-Andujar, D.-V. Nguyen, C. Affolter, S. Boutry, A. Boos, P. Ronot, B. Uring-Lambert, P. Choquet, P. E. Zorn, D. Mertz, S. Laurent, R. N. Muller, F. Meyer, D. F. Flesch, S. Begin-Colin, *Nanotechnology* **2019**, *30*, 374002.
- [20] D. Mertz, O. Sandre, S. Bégin-Colin, *Biochimica et Biophysica Acta (BBA) - General Subjects* **2017**, *1861*, 1617–1641.
- [21] D.-H. Kim, Y. Guo, Z. Zhang, D. Procissi, J. Nicolai, R. A. Omary, A. C. Larson, *Adv Healthc Mater* **2014**, *3*, 714–724.
- [22] A. K. Gaharwar, J. E. Wong, D. Müller-Schulte, D. Bahadur, W. Richtering, “Magnetic Nanoparticles Encapsulated Within a Thermoresponsive Polymer,” DOI 10.1166/jnn.2009.1265 can be found under <https://www.ingentaconnect.com/contentone/asp/jnn/2009/00000009/00000009/art00041>, **2009**.
- [23] M. Bordawekar, G. G. Lipscomb, I. Escobar, *Separation Science and Technology* **2009**, *44*, 3369–3391.
- [24] J. M. Van Alstine, N. L. Burns, J. A. Riggs, K. Holmberg, J. M. Harris, *Colloids and Surfaces A: Physicochemical and Engineering Aspects* **1993**, *77*, 149–158.
- [25] M. H. Turabee, T. H. Jeong, P. Ramalingam, J. H. Kang, Y. T. Ko, *Carbohydrate Polymers* **2019**, *203*, 302–309.
- [26] K. Al Khateb, E. K. Ozhmukhametova, M. N. Mussin, S. K. Seilkhanov, T. K. Rakhypbekov, W. M. Lau, V. V. Khutoryanskiy, *International Journal of Pharmaceutics* **2016**, *502*, 70–79.
- [27] B. Liu, C. Chen, W. Zhang, J. Crittenden, Y. Chen, *Desalination* **2012**, *307*, 26–33.

- [28] Y. Wang, T. Wang, Y. Su, F. Peng, H. Wu, Z. Jiang, *Langmuir* **2005**, *21*, 11856–11862.
- [29] W. Zhao, Y. Su, C. Li, Q. Shi, X. Ning, Z. Jiang, *Journal of Membrane Science* **2008**, *318*, 405–412.